J. Fluid Mech. (2012), *vol.* 704, *pp.* 109–136. © Cambridge University Press 2012
doi:10.1017/jfm.2012.221

Streaming-potential phenomena in the thin-Debye-layer limit. Part 2. Moderate Péclet numbers

Ory Schnitzer[1], Itzchak Frankel[2] and Ehud Yariv[1]†

[1] Department of Mathematics, Technion – Israel Institute of Technology, Haifa 32000, Israel

[2] Department of Aerospace Engineering, Technion – Israel Institute of Technology, Haifa 32000, Israel

(Received 5 January 2012; revised 9 April 2012; accepted 7 May 2012;
first published online 3 July 2012)

Macroscale description of streaming-potential phenomena in the thin-double-layer limit, and in particular the associated electro-viscous forces, has been a matter of long-standing controversy. In part 1 of this work (Yariv, Schnitzer & Frankel, *J. Fluid Mech.*, vol. 685, 2011, pp. 306–334) we identified that the product of the Hartmann (λ) and Péclet (Pe) numbers is $O(\delta^{-2})$, δ being the dimensionless Debye thickness. This scaling relationship defines a one-family class of limit processes appropriate to the consistent analysis of this singular problem. In that earlier contribution we focused on the generic problems associated with moderate λ and large Pe, where the streaming-potential magnitude is comparable to the thermal voltage. Here we consider the companion generic limit of moderate Péclet numbers and large Hartmann numbers, deriving the appropriate macroscale model wherein the Debye-layer physics is represented by effective boundary conditions. Since the induced electric field is asymptotically smaller, calculation of these conditions requires higher asymptotic orders in analysing the Debye-scale transport. Nonetheless, the leading-order electro-viscous forces are of the same $O(\delta^2)$ relative magnitude as those previously obtained in the large-Pe limit. The structure of these forces is different, however, first because the small Maxwell stresses do not contribute at leading order, and second because salt polarization results in a dominant diffuso-osmotic slip. Since the salt distribution is governed by an advection–diffusion equation, this slip gives rise to electro-viscous forces which are nonlinear in the driving flow. The resulting scheme is illustrated by the calculation of the electro-viscous excess drag in the prototype problem of a translating sphere.

Key words: colloids, low-Reynolds-number flows

1. Introduction

1.1. *Background*

Streaming-potential phenomena in the limit of thin double layers were originally addressed by Smoluchowski (1921), who considered what may be the simplest problem in this field: a sphere translating through an unbounded fluid domain. Using a heuristic approach, Smoluchowski predicted an electro-viscous drag enhancement

† Email address for correspondence: udi@technion.ac.il

https://doi.org/10.1017/jfm.2012.221 Published online by Cambridge University Press

over the classical Stokes law. Following Overbeek (1943), electrokinetic effects were analysed in a more systematic manner, using the Poisson–Nernst–Planck framework (the 'standard model'). The excess drag on a moving sphere was thereby calculated for arbitrary Debye thickness using two different approximations: small zeta potentials (Booth 1954) and weak gravity (Ohshima *et al.* 1984). These analyses typically lagged several years behind the corresponding approximations for *field-driven* electrophoresis of a spherical particle for small zeta potentials (Booth 1950) and weak applied fields (O'Brien & White 1978).

Interestingly, the ubiquitous limit of thin double layers was addressed rather late within the standard model. Perhaps this may have to do with the need to use matched asymptotic expansions (Yariv 2010). Here one readily notices a major difference between field-driven electrokinetic phenomena, where the thin-double-layer limit is well understood (Morrison 1970; Prieve *et al.* 1984; Keh & Anderson 1985; Rubinstein & Zaltzman 2001; Yariv 2010) and *flow-driven* (i.e. streaming-potential) phenomena, where the appropriate thin-Debye-layer limit has been a matter of long-standing controversy.

In the latter class, the pioneering contribution is that of Ohshima *et al.* (1984), who obtained the thin-Debye-layer limit as a degenerate case of the weak-gravity analysis (performed for arbitrary Debye-layer thickness). The first treatment of generic geometries in that limit was carried out by Bike & Prieve (1992). Their model reflected the generation of bulk electric fields owing to the non-uniform 'streaming' advective currents within the Debye layer. The resulting electro-viscous forces were exclusively attributed to the accompanying Maxwell stresses, entirely neglecting the perturbation to the original 'driving flow'. For the prototype problem of a sedimenting sphere, this model clearly explains the generation of electric field by imposed motion, but fails to predict any excess drag.

Motivated by the experiments of Alexander & Prieve (1987), similar models have been applied to the calculation of the electro-viscous force on a particle moving parallel to to a planar wall (Bike & Prieve 1990; van de Ven, Warszynski & Dukhin 1993). Again neglecting the hydrodynamic contribution, the electro-viscous model has predicted a lift force normal to the wall, in agreement with experimental observations. The magnitude of the predicted force, however, underestimates the measured values by orders of magnitudes.

The above controversies were apparently settled by the seminal generic analysis of Cox (1997) based on systematic matched asymptotic expansions. His dimensionless formulation essentially entails three parameters: the Debye thickness δ; the Péclet number Pe, representing the relative magnitude of ionic advection and diffusion; and a Hartmann-type number λ, essentially representing the relative magnitude of Coulomb body forces and viscous stresses. Assuming that δ is small while the Hartmann and Péclet numbers are both $O(1)$, Cox (1997) has obtained $O(\delta^6)$ Maxwell stresses, while the viscous stresses associated with the flow perturbation, neglected by Bike & Prieve (1992), are predicted $O(\delta^4)$. For small Péclet numbers, Cox also managed to calculate the excess drag on a sedimenting particle, the result being in agreement with the weak-gravity expression of Ohshima *et al.* (1984). Following Cox (1997), the problem of electrokinetic lift has been revisited using more detailed electrokinetic models, which take into account both Maxwell and Newtonian stresses (Warszyski, Wu & van de Ven 1998; Tabatabaei, van de Ven & Rey 2006).

The problem of streaming-potential phenomena in the thin-double-layer limit was also addressed by Dukhin (1993). We do not understand the underlying assumptions in

https://doi.org/10.1017/jfm.2012.221 Published online by Cambridge University Press

his analysis, nor the principles of his calculations. In any event, it does not seem that his work is focused on obtaining a macroscale description.

1.2. *Oversight in Cox (1997), and the moderate-Hartmann-number limit*

In a recent paper (Yariv, Schnitzer & Frankel 2011), hereafter referred to as part 1, we identified an oversight in Cox (1997). Specifically, we demonstrated that in the thin-Debye-layer limit the product of the Hartmann and Péclet numbers scales as δ^{-2}: see (2.4). It is therefore clear that these two numbers cannot both be $O(1)$ in that limit, in contrast to the explicit assumption and scaling employed by Cox (1997). (The assumption of small Péclet number when solving specific configurations further aggravates this contradiction.)

The scaling analysis in part 1 shows that the induced streaming potential in the bulk becomes comparable to the thermal voltage when the Hartmann number is $O(1)$. Most of part 1 thus focuses on that asymptotic limit, where the Péclet number Pe is $O(\delta^{-2})$ large. The need to address $O(\delta^{-2})$ Péclet numbers was hinted at in the review paper by Saville (1977), where he wrote: 'For larger Péclet numbers it turns out that a solution is possible using singular-perturbation methods for $\delta \ll 1$ as long as $Pe\,\delta^2$ stays $O(1)$ (Saville unpublished).'

The dominant advection at these Péclet numbers leads to a substantial simplification of the macroscale description, as compared with Cox's scheme. Moreover, the electro-viscous forces become $O(\delta^2)$ in that limit, and are contributed by both the electric field (through Maxwell stresses) and the velocity perturbation (through viscous stresses). For the prototype problem of a translating sphere, Yariv *et al.* (2011) obtained an excess drag different to that obtained by Cox (1997) – actually recovering Smoluchowski's result.

1.3. *Moderate Péclet numbers*

Since the Péclet number is set externally by the imposed flow, it may vary across a wide range of values. One may therefore consider possible limits other than that above which are consistent with the scaling analysis of part 1. (The link between the Péclet and Hartmann numbers represents a one-parametric class of consistent limit processes.) The procedure of fixing the Hartmann number by setting the corresponding value of the Péclet number is compatible with the typical experimental setup where one achieves the thin-Debye-layer limit by increasing the salt concentration, with the Péclet number essentially remaining fixed.

Typical streaming-potential phenomena are, roughly speaking, divided into shear-driven flows and sedimentation problems, respectively. In shear-driven flows, where the velocity scale is directly controlled, one can in principle achieve large Péclet numbers. This is less so in sedimentation problems, where the settling velocity is controlled rather indirectly, by the choice of particle size and excess density. Consider for instance the sedimentation of a particle of typical dimension a^* and excess density ρ^* in a liquid electrolyte of viscosity μ^* and ionic diffusivity D^*. The particle velocity v^* is of order $2\rho^* g^* a^{*2}/9\mu^*$, g^* being the acceleration due to gravity, whereby the Péclet number is $Pe = 2\rho^* g^* a^{*3}/9\mu^* D^*$. For typical 20 μm polystyrene particles ($\rho^* \approx 50$ kg m^{-3}) at aqueous electrolytes ($\mu \approx 10^{-3}$ kg m^{-1} s^{-1}, $D^* \approx 10^{-9}$ m^2 s^{-1}) we find $Pe \approx 1$. It is therefore important to theoretically consider the limit $Pe \sim O(1)$ (where the Hartmann number is $O(\delta^{-2})$: see (2.4)). The goal of the present paper is to derive a generic macroscale description in this limit, where, as in part 1, the effective boundary conditions result from asymptotic matching between the 'outer' electro-neutral bulk and the 'inner' Debye-layer fields.

https://doi.org/10.1017/jfm.2012.221 Published online by Cambridge University Press

This present limit is fundamentally different from that of large Péclet numbers, which was the focus of part 1. With $Pe \sim O(1)$, ionic advection within the Debye layer will only emerge at $O(\delta)$ in the Nernst–Planck equations (as opposed to $O(\delta^{-1})$ at the large-Pe limit: see part 1). Convection-induced ionic currents, constituting the first deviation from a Boltzmann distribution, therefore appear only at $O(\delta^2)$. This implies the need to go to higher asymptotic orders when seeking the electro-viscous effect. Nevertheless, this effect still turns out to be $O(\delta^2)$, as in the large-Pe limit. Because the induced field is weak (see (2.6)) the quadratic Maxwell stresses do not contribute to that asymptotic order. Unlike the large-Péclet limit, the moderate advection associated with $O(1)$ Péclet numbers does not mandate here a uniform salt distribution in the electro-neutral bulk.

This paper is arranged as follows. For easy reference we summarize in the next section the generic formulation of the streaming-potential problem already derived in part 1. For simplicity, we initially focus on problems which are steady in a reference frame where the solid walls are stationary. The analysis of the 'electro-neutral' outer region is presented in § 3. The formulation of the inner problem within the Debye layer is outlined in § 4, and its analysis is performed in § 5. The slip condition governing the outer velocity perturbation is derived in § 6; the Neumann conditions governing the outer salt and electric-potential perturbations are derived in § 7. In § 8 the generic scheme is extended to unsteady problems. The resulting macroscale scheme is summarized in § 9; it is illustrated in § 10 for the problem of a translating particle. Concluding comments appear in § 11.

Readers who are not interested in the mathematical derivation of the macroscale model can skip directly from § 3 to § 9.

2. Generic formulation

2.1. *Non-dimensionalization and scaling*

The generic statement of the streaming-potential problem (see part 1) is reiterated here for easy reference. We consider the electrokinetic transport occurring within a symmetric binary electrolyte solution (valencies $\pm\mathscr{Z}$, dielectric permittivity ϵ^*, viscosity μ^*) which is driven by an imposed flow (of typical speed v^*) relative to a charged solid wall. The typical linear dimension of the system (characterizing e.g. the solid wall or the imposed flow) is denoted a^*. Focusing on flow-driven phenomena, no electric field or salt gradients are imposed. Thus, at large distances away from the wall the electric field vanishes and the two ionic concentrations approach the equilibrium value c^*.

Three parameters readily emerge in the dimensionless description of part 1. The Péclet number

$$Pe = \frac{a^* v^*}{D^*}, \tag{2.1}$$

in which D^* is the (presumed equal) diffusivity of the two ionic species, represents the ratio of ionic advection and diffusion in the Nernst–Planck equations (see (2.7)). Poisson's equation (see (2.9)) introduces the dimensionless Debye thickness δ, defined by

$$\delta^2 = \frac{\epsilon^* \varphi^*}{2\mathscr{Z} e^* a^{*2} c^*}, \tag{2.2}$$

https://doi.org/10.1017/jfm.2012.221 Published online by Cambridge University Press

in which $\varphi^* = k^*T^*/\mathscr{Z}e^*$ is the thermal voltage (wherein k^*T^* is the Boltzmann temperature and e^* the elementary charge). Lastly, the Hartmann number,

$$\lambda = \frac{2k^*T^*a^*c^*}{\mu^*v^*}, \tag{2.3}$$

characterizes the relative magnitude of electrical body forces in the fluid momentum balance.

The key observation of part 1 is that the above three parameters are not independent. Rather, the following scaling relation holds:

$$\lambda = \frac{\alpha}{Pe}\delta^{-2}, \tag{2.4}$$

in which the dimensionless ion-drag coefficient

$$\alpha = \frac{\epsilon^*\varphi^{*2}}{\mu^*D^*} \tag{2.5}$$

is independent of both particle dimension a^* and electrolyte concentration c^*. For typical ionic diffusivities ($D^* \approx 10^{-9}$ m^2 s^{-1}) in aqueous solutions ($\mu^* \approx 10^{-3}$ kg m^{-1} s^{-1}), $\alpha \approx 0.5$. By the Stokes–Einstein relation, (2.5) is independent of μ^*, whence α is of order unity for highly viscous solutions as well. Saville (1977) interpreted α as a Péclet number; indeed, in field-driven phenomena α multiplies the advection term in the ion-conservation equation and thus plays this role when the applied field is comparable with φ^*/a^*. In flow-driven phenomena, this interpretation ceases to hold: see (2.7).

Another dimensionless parameter, β, represents the ratio of the induced field in the bulk to the thermal scale φ^*/a^*. A scaling analysis in part 1 shows that

$$\beta = Pe\,\delta^2. \tag{2.6}$$

In the present paper, where we consider $O(1)$ Péclet numbers, we accordingly anticipate $O(\delta^2)$ bulk fields (see (3.3)). This is in contrast with the single voltage scale existing at $O(\delta^{-2})$ Péclet numbers.

Finally, we neglect at the outset the effect of fluid inertia. With typical values of ionic diffusivity the Schmidt number is easily of order 10^3: it is thus *a priori* obvious that, for $Pe \sim O(1)$, the Reynolds number is small.

2.2. *Governing equations*

The governing equations are presented in a wall-fixed reference system. For simplicity we initially consider situations where the problem is time-independent in this system. (This assumption is relaxed in § 8.) We employ the dimensionless notation of part 1, with length variables normalized by a^*, the ionic concentrations $c^{\pm}$ by the equilibrium value c^*, the electric potential φ by the thermal voltage φ^*, the velocity field $\boldsymbol{v}$ by v^* and the pressure p (and the stress) by μ^*v^*/a^*.

The differential equations consist of (i) the Nernst–Planck equations

$$\boldsymbol{\nabla}\cdot\boldsymbol{j}^{\pm} + Pe\,\boldsymbol{v}\cdot\boldsymbol{\nabla}c^{\pm} = 0, \tag{2.7}$$

wherein

$$\boldsymbol{j}^{\pm} = \mp c^{\pm}\boldsymbol{\nabla}\varphi - \boldsymbol{\nabla}c^{\pm} \tag{2.8}$$

are the molecular ionic fluxes, (ii) Poisson's equation

$$\delta^2\nabla^2\varphi = -q, \tag{2.9}$$

https://doi.org/10.1017/jfm.2012.221 Published online by Cambridge University Press

and (iii) the continuity and inhomogeneous Stokes equations

$$\boldsymbol{\nabla}\cdot\boldsymbol{v}=0, \tag{2.10}$$

$$\nabla^2\boldsymbol{v}-\boldsymbol{\nabla}p=\lambda q\boldsymbol{\nabla}\varphi, \tag{2.11}$$

accounting for Coulomb body forces. The quantity

$$q=\tfrac{1}{2}(c^+-c^-) \tag{2.12}$$

appearing in (2.9) and (2.13) is the volumetric charge density, normalized by $2\mathscr{Z}e^*c^*$. Substitution of (2.4) yields the alternative form of the Stokes equations,

$$\nabla^2\boldsymbol{v}-\boldsymbol{\nabla}p=\delta^{-2}\frac{\alpha}{Pe}q\boldsymbol{\nabla}\varphi, \tag{2.13}$$

expressed in terms of Pe rather than λ.

An alternative description of ionic conservation is obtained using (2.12) and the mean ('salt') concentration

$$c=\tfrac{1}{2}(c^+ + c^-). \tag{2.14}$$

Thus, addition of (2.7) yields the salt balance

$$\boldsymbol{\nabla}\cdot\boldsymbol{j}+Pe\,\boldsymbol{v}\cdot\boldsymbol{\nabla}c=0, \tag{2.15}$$

wherein

$$\boldsymbol{j}=\tfrac{1}{2}(\boldsymbol{j}^+ +\boldsymbol{j}^-)=-q\boldsymbol{\nabla}\varphi-\boldsymbol{\nabla}c \tag{2.16}$$

is the salt flux. Similarly, subtraction of these equations provides the charge balance

$$\boldsymbol{\nabla}\cdot\boldsymbol{i}+Pe\,\boldsymbol{v}\cdot\boldsymbol{\nabla}q=0, \tag{2.17}$$

wherein

$$\boldsymbol{i}=\tfrac{1}{2}(\boldsymbol{j}^+ -\boldsymbol{j}^-)=-c\boldsymbol{\nabla}\varphi-\boldsymbol{\nabla}q \tag{2.18}$$

is the current density.

2.3. *Boundary conditions*

The boundary conditions on the stationary solid surface (generically denoted as S) are specified in terms of the unit normal $\hat{\boldsymbol{n}}$ pointing into the fluid. They comprise: (i) the impermeability and no-slip conditions

$$\boldsymbol{v}=\boldsymbol{0}\quad\text{on } S, \tag{2.19}$$

(ii) the no-flux conditions

$$\hat{\boldsymbol{n}}\cdot\boldsymbol{j}_\pm=0\quad\text{on } S, \tag{2.20}$$

which may be written alternatively as

$$\hat{\boldsymbol{n}}\cdot\boldsymbol{j}=0,\quad \hat{\boldsymbol{n}}\cdot\boldsymbol{i}=0\quad\text{on } S, \tag{2.21a,b}$$

and (iii) Gauss's boundary condition, relating the electric displacements in both the liquid and solid media to σ, the generally non-uniform surface-charge density (normalized by $\epsilon^*\kappa^*\varphi^*$) on S,

$$\frac{\partial\varphi}{\partial n}=-\delta^{-1}\sigma+\gamma\frac{\partial\bar{\varphi}}{\partial n}\quad\text{on } S. \tag{2.22}$$

https://doi.org/10.1017/jfm.2012.221 Published online by Cambridge University Press

Here $\partial/\partial n = \hat{\boldsymbol{n}} \cdot \boldsymbol{\nabla}$, $\bar{\varphi}$ is the electric potential in the solid wall, and γ is the ratio of the respective dielectric constants in the solid and liquid phases. In principle, this condition couples the fluid problem to the electrostatic problem within the charge-free solid wall, consisting of Laplace's equation governing $\bar{\varphi}$ and the condition of electric-potential continuity

$$\bar{\varphi} = \varphi \quad \text{on } S. \tag{2.23}$$

At large distances away from the wall, the ionic concentrations approach their equilibrium values, whereby

$$c \to 1, \quad q \to 0 \quad \text{as } |\boldsymbol{x}| \to \infty. \tag{2.24a,b}$$

At these distances the electric field vanishes,

$$\boldsymbol{\nabla}\varphi \to \boldsymbol{0} \quad \text{as } |\boldsymbol{x}| \to \infty, \tag{2.25}$$

and the velocity field approaches the externally imposed flow, say $\boldsymbol{v}_\infty(\boldsymbol{x})$ (a solution of the Stokes equations),

$$\boldsymbol{v} \sim \boldsymbol{v}_\infty(\boldsymbol{x}) \quad \text{as } |\boldsymbol{x}| \to \infty. \tag{2.26}$$

2.4. *Forces and torques*

It is common for the solid wall to represent the boundary of one or more particles suspended in an electrolyte solution. Whether the particles are freely suspended (i.e. a 'mobility' problem) or else constrained to move in a prescribed manner, the resultant force and torque on each particle are usually required. The force (normalized by $\mu^* v^* a^*$) is obtained by integrating the stresses over the particle boundary S,

$$\boldsymbol{F} = \oint_S \mathrm{d}A\, \hat{\boldsymbol{n}} \cdot (\boldsymbol{N} + \boldsymbol{M}), \tag{2.27}$$

where $\boldsymbol{N}$ is the Newtonian Cauchy stress

$$\boldsymbol{N} = -p\boldsymbol{I} + (\boldsymbol{\nabla}\boldsymbol{v}) + (\boldsymbol{\nabla}\boldsymbol{v})^{\mathrm{T}} \tag{2.28}$$

($\boldsymbol{I}$ being the idemfactor and T denoting dyadic transposition) and $\boldsymbol{M}$ the Maxwell stress

$$\boldsymbol{M} = \frac{\alpha}{Pe}\left(\boldsymbol{\nabla}\varphi\boldsymbol{\nabla}\varphi - \frac{1}{2}\boldsymbol{\nabla}\varphi \cdot \boldsymbol{\nabla}\varphi\, \boldsymbol{I}\right). \tag{2.29}$$

Similarly, the torque (normalized by $\mu^* v^* a^{*2}$) experienced by a particle about the point $\boldsymbol{x}_0$ is

$$\boldsymbol{T} = \oint_S \mathrm{d}A\, (\boldsymbol{x} - \boldsymbol{x}_0) \times \left[\hat{\boldsymbol{n}} \cdot (\boldsymbol{N} + \boldsymbol{M})\right]. \tag{2.30}$$

Since the momentum balance equation (2.13) represents a statement of divergence-free stress,

$$\boldsymbol{\nabla} \cdot (\boldsymbol{N} + \boldsymbol{M}) = 0, \tag{2.31}$$

use of Gauss's theorem allows for evaluation of (2.27) and (2.30) over any surface enclosing S which lies entirely within the fluid (and does not enclose another particle).

https://doi.org/10.1017/jfm.2012.221 Published online by Cambridge University Press

2.5. *Thin-double-layer limit*

Our goal is to analyse this generic problem in the thin-Debye-layer limit

$$\delta \ll 1. \tag{2.32}$$

Since this limit is singular (see (2.9)), we employ at the outset matched asymptotic expansions, separately analysing the $O(\delta)$-wide 'inner' Debye layer adjacent to S and the 'outer' electro-neutral bulk outside it. As in part 1, our goal is to derive a reduced macroscale model for the bulk domain, with the effective boundary conditions resulting from asymptotic matching with the Debye fields. We denote by s the macroscale boundary corresponding to the outer edge of the Debye layer to distinguish it from the true solid–liquid interface S.

3. Outer analysis

The appearance of the small parameter δ^2 in both (2.9) and (2.13) suggests the generic expansion

$$f(\boldsymbol{x};\delta) \sim f_0(\boldsymbol{x}) + \delta^2 f_2(\boldsymbol{x}) + \cdots. \tag{3.1}$$

Poisson's equation (2.9) yields the leading-order electro-neutrality

$$q_0 \equiv 0. \tag{3.2}$$

In view of the scaling relation (2.6), we anticipate that bulk electric fields appear only at $O(\delta^2)$,

$$\varphi_0 \equiv 0. \tag{3.3}$$

We also anticipate uniform salt distribution at leading order, whereby condition (2.24*a*) implies

$$c_0 \equiv 1. \tag{3.4}$$

(Subsequent analysis indeed demonstrates that salt polarization only appears at higher asymptotic orders.) Equations (3.3)–(3.4) are compatible with (3.2) and (2.15)–(2.18) and with the far-field conditions (2.24)–(2.25). These predictions must still be confirmed *a posteriori* via matching with the inner fields.

With leading-order electro-neutrality and (3.3), (2.10)–(2.13) yield at leading order the homogeneous Stokes equations

$$\boldsymbol{\nabla}\cdot\boldsymbol{v}_0 = 0, \quad \boldsymbol{\nabla} p_0 = \nabla^2 \boldsymbol{v}_0. \tag{3.5a,b}$$

Anticipating small fluid velocities near the presumed stationary walls, we postulate the effective boundary condition (cf. (2.19))

$$\boldsymbol{v}_0 = \boldsymbol{0} \quad \text{on } s, \tag{3.6}$$

which must be verified *a posteriori* via asymptotic matching with the inner velocity.

At the next asymptotic level, we note that (3.3) together with Poisson's equation (2.9) yields

$$q_2 \equiv 0. \tag{3.7}$$

Substitution of (3.2)–(3.4) and (3.7) into (2.16) and (2.18) yields

$$\boldsymbol{j}_2 = -\boldsymbol{\nabla} c_2, \quad \boldsymbol{i}_2 = -\boldsymbol{\nabla}\varphi_2. \tag{3.8a,b}$$

https://doi.org/10.1017/jfm.2012.221 Published online by Cambridge University Press

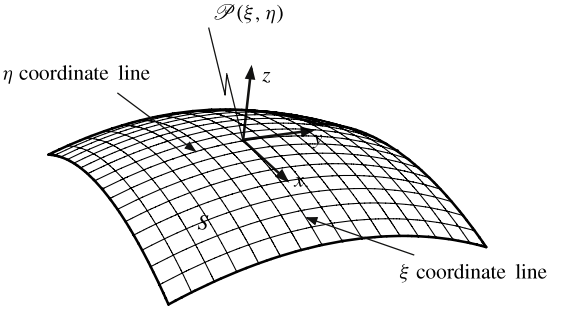


FIGURE 1. Schematic definition of the curvilinear surface coordinates (η, ξ) parametrizing S and the local Cartesian system (x, y, z) centred about an arbitrary surface point $\mathscr{P}$.

Thus, the salt balance equation (2.15) yields

$$\nabla^2 c_2 = Pe\, \boldsymbol{v}_0 \cdot \boldsymbol{\nabla} c_2, \tag{3.9}$$

while the charge balance equation (2.17) yields

$$\nabla^2 \varphi_2 = 0. \tag{3.10}$$

With electro-neutrality valid up to $O(\delta^2)$, and in view of (3.3), we find from (2.10)–(2.13) that the flow perturbation is also governed by the homogeneous Stokes equation

$$\boldsymbol{\nabla} \cdot \boldsymbol{v}_2 = 0, \quad \boldsymbol{\nabla} p_2 = \nabla^2 \boldsymbol{v}_2. \tag{3.11a,b}$$

Note that all $O(\delta^2)$ fields must vanish at infinity. Furthermore, they must match the corresponding inner fields.

4. Inner formulation

4.1. *Cartesian and curvilinear coordinates*

In analysing the inner-region transport, we employ Cox's method to describe the domain adjacent to the (generally curved) solid surface. Thus, we employ locally orthogonal curvilinear coordinates (ξ, η) possessing unity metric coefficients, such that $\hat{\boldsymbol{e}}_\xi \times \hat{\boldsymbol{e}}_\eta$ is normal to S, pointing into the liquid. At any arbitrary point $\mathscr{P}$ on S a local Cartesian system (x, y, z) is constructed by choosing the x and y coordinate axes tangent to the ξ and η coordinate lines, respectively, with the origin at $\mathscr{P}$. With this choice, the z-axis points into the fluid in a direction normal to S: see figure 1.

Near $\mathscr{P}$ the Debye layer is described by the rescaled inner coordinates (X, Y, Z), defined by

$$x = \delta^{1/2} X, \quad y = \delta^{1/2} Y, \quad z = \delta Z. \tag{4.1a,b,c}$$

When applying the boundary conditions, it is useful to identify S with a coordinate surface. In the present description, the plane $Z = 0$ is only a leading-order approximation to S. The ingenious procedure of Cox (1997) consists of seeking the inner fields only at $X = Y = 0$, while the dependence on position on S is implicit in the pair (ξ, η) used to parametrize $\mathscr{P}$. With this interpretation, S is described by $Z = 0$. Of course, one now needs appropriate transformations between partial derivatives with

https://doi.org/10.1017/jfm.2012.221 Published online by Cambridge University Press

respect to X and Y and those with respect to ξ and η. For $X = Y = 0$ Cox obtained

$$\left.\frac{\partial F}{\partial X}\right|_{X=Y=0} = \delta^{1/2}\frac{\partial F}{\partial \xi} + \cdots, \quad \left.\frac{\partial F}{\partial Y}\right|_{X=Y=0} = \delta^{1/2}\frac{\partial F}{\partial \eta} + \cdots, \tag{4.2a,b}$$

as well as

$$\left(\frac{\partial^2}{\partial X^2} + \frac{\partial^2}{\partial Y^2}\right) F\Big|_{X=Y=0} = (\boldsymbol{\nabla}\cdot\hat{\boldsymbol{n}})\frac{\partial F}{\partial Z} + \cdots, \tag{4.3}$$

with $\boldsymbol{\nabla}\cdot\hat{\boldsymbol{n}}$ being the dimensionless sum of the principal curvatures. In these transformations, the error terms are of $O(\delta)$ relative magnitude.

4.2. *Field scaling and governing equations*

Inner fields are denoted by capital letters. Specifically, for each generic field f we define $f = \delta^n F$ with n chosen so that F is $O(1)$. Thus, different scalings are required for the Cartesian components (u, v, w) of $\boldsymbol{v}$: the no-slip condition (2.19) suggests that the tangential components constitute an extrapolation of the outer flow,

$$u = \delta U, \quad v = \delta V. \tag{4.4a,b}$$

These, in conjunction with the continuity equation and impermeability on S, suggest that

$$w = \delta^2 W. \tag{4.5}$$

This scaling is consistent with the effective no-slip condition (3.6), as can be verified by a 1–1 Van Dyke matching procedure (Van Dyke 1964). The present velocity scaling differs from that in field-driven phenomena, where the non-conservative Coulomb body forces induce an $O(1)$ tangential flow. Here, in the absence of external fields, Coulomb forces are conservative at the leading asymptotic orders, and are hence balanced by an 'osmotic' pressure. Specifically, the large Coulomb forces in (2.13) imply an $O(\delta^{-2})$ pressure,

$$p = \delta^{-2} P. \tag{4.6}$$

No rescaling is needed for the electric potential and ionic concentrations,

$$\varphi = \Phi, \quad c^{\pm} = C^{\pm}, \tag{4.7a,b}$$

so we simply define

$$c = C, \quad q = Q. \tag{4.8a,b}$$

With the above re-scaling, the Nernst–Planck equations (2.7) become

$$\delta^{-2}\frac{\partial J_Z^{\pm}}{\partial Z} + \delta^{-1}\left(\frac{\partial J_X^{\pm}}{\partial X} + \frac{\partial J_Y^{\pm}}{\partial Y}\right) + \delta\, Pe\left(\delta^{-1/2}U\frac{\partial C^{\pm}}{\partial X} + \delta^{-1/2}V\frac{\partial C^{\pm}}{\partial Y} + W\frac{\partial C^{\pm}}{\partial Z}\right) = 0, \tag{4.9}$$

in which

$$J_Z^{\pm} = -\frac{\partial C^{\pm}}{\partial Z} \mp C^{\pm}\frac{\partial \Phi}{\partial Z} \tag{4.10}$$

represent $O(\delta^{-1})$ fluxes in the z-direction and

$$J_X^{\pm} = -\frac{\partial C^{\pm}}{\partial X} \mp C^{\pm}\frac{\partial \Phi}{\partial X} \tag{4.11}$$

https://doi.org/10.1017/jfm.2012.221 Published online by Cambridge University Press

represent $O(\delta^{-1/2})$ fluxes in the x-direction, with similar expressions defining $J_Y^{\pm}$ (see however (7.1) *et seq.*). Poisson's equation (2.9) becomes

$$\frac{\partial^2 \Phi}{\partial Z^2} + \delta\left(\frac{\partial^2 \Phi}{\partial X^2} + \frac{\partial^2 \Phi}{\partial Y^2}\right) = Q. \tag{4.12}$$

The momentum balance equation (2.13) in the z-direction reads

$$\delta^{-3}\left(\frac{\partial P}{\partial Z} + \frac{\alpha}{Pe} Q \frac{\partial \Phi}{\partial Z}\right) = \frac{\partial^2 W}{\partial Z^2} + \delta\left(\frac{\partial^2 W}{\partial X^2} + \frac{\partial^2 W}{\partial Y^2}\right), \tag{4.13}$$

while that in the x-direction reads

$$\delta^{-2}\left(\delta^{-1/2}\frac{\partial P}{\partial X} + \delta^{-1/2}\frac{\alpha}{Pe} Q \frac{\partial \Phi}{\partial X}\right) = \delta^{-1}\frac{\partial^2 U}{\partial Z^2} + \left(\frac{\partial^2 U}{\partial X^2} + \frac{\partial^2 U}{\partial Y^2}\right) \tag{4.14}$$

(with a similar equation for the y-direction). Lastly, the continuity equation (2.10) becomes

$$\delta^{-1/2}\left(\frac{\partial U}{\partial X} + \frac{\partial V}{\partial Y}\right) + \frac{\partial W}{\partial Z} = 0. \tag{4.15}$$

In principle, the derivatives with respect to X and Y should be transformed using (4.2)–(4.3). However, these derivatives only show up at the highest order in our analysis. We accordingly defer these transformation to derivatives with respect to ξ and η, postponing the introduction of the unknown error terms in (4.2)–(4.3) that would otherwise hinder progress beyond leading-order analysis.

Using Cox's representation, the solid boundary coincides with the surface $Z = 0$. In terms of the velocity components, condition (2.19) consists of both fluid impermeability

$$W = 0 \tag{4.16}$$

and no-slip

$$U = V = 0. \tag{4.17}$$

Condition (2.20) becomes

$$J_Z^{\pm} = 0. \tag{4.18}$$

Lastly, Gauss's boundary condition (2.22) now reads

$$\frac{\partial \Phi}{\partial Z} = -\sigma + \delta\gamma\frac{\partial \bar{\varphi}}{\partial n}. \tag{4.19}$$

Since no comparable Debye layer is established in the solid phase, the electric displacement within the solid turns out to be of $O(\delta)$ relative magnitude. Here we assume that $\gamma = O(1)$. In principle, this displacement would shift to leading order for extremely large dielectric permittivities of the solid, where $\gamma = O(\delta^{-1})$ (Yossifon, Frankel & Miloh 2007; Yariv & Davis 2010); for common dielectric solids prevailing in experiments (glass, polystyrene, etc.), however, γ is actually small.

4.3. *Asymptotic expansions and large-Z conditions*

The inner fields are now expanded in powers of δ, with the indices reflecting the original scaling (4.4)–(4.6). Thus, the velocity components are expanded as

$$U \sim U_1 + \delta U_2 + \cdots, \quad V \sim V_1 + \delta V_2 + \cdots, \quad W \sim W_2 + \cdots, \tag{4.20a,b,c}$$

https://doi.org/10.1017/jfm.2012.221 Published online by Cambridge University Press

while the electric potential and ionic concentrations possess the expansions

$$\Phi \sim \Phi_0 + \delta\Phi_1 + \delta^2\Phi_2 + \cdots, \tag{4.21}$$

$$C^{\pm} \sim C_0^{\pm} + \delta C_1^{\pm} + \delta^2 C_2^{\pm} + \cdots, \tag{4.22}$$

the latter implying

$$C \sim C_0 + \delta C_1 + \delta^2 C_2 + \cdots, \quad Q \sim Q_0 + \delta Q_1 + \delta^2 Q_2 + \cdots. \tag{4.23a,b}$$

The pressure and normal fluxes are expanded as

$$P \sim P_{-2} + \delta P_{-1} + \delta^2 P_0 + \cdots, \tag{4.24}$$

$$J_Z^{\pm} \sim J_{Z,-1}^{\pm} + \delta J_{Z,0}^{\pm} + \delta^2 J_{Z,1}^{\pm} + \delta^3 J_{Z,2}^{\pm} + \cdots, \tag{4.25}$$

wherein

$$\left.\begin{aligned} J_{Z,-1}^{\pm} &\sim -\frac{\partial C_0^{\pm}}{\partial Z} \mp C_0^{\pm}\frac{\partial \Phi_0}{\partial Z}, \\ J_{Z,0}^{\pm} &\sim -\frac{\partial C_1^{\pm}}{\partial Z} \mp C_0^{\pm}\frac{\partial \Phi_1}{\partial Z} \mp C_1^{\pm}\frac{\partial \Phi_0}{\partial Z}, \\ J_{Z,1}^{\pm} &\sim -\frac{\partial C_2^{\pm}}{\partial Z} \mp C_0^{\pm}\frac{\partial \Phi_2}{\partial Z} \mp C_1^{\pm}\frac{\partial \Phi_1}{\partial Z} \mp C_2^{\pm}\frac{\partial \Phi_0}{\partial Z}, \\ &\cdots \end{aligned}\right\} \tag{4.26}$$

Clearly, the homogeneous boundary conditions (4.16)–(4.18) separately apply to each term in expansions (4.20) and (4.25). Also, matching with the leading-order outer fields (3.2)–(3.4) implies

$$C_0^{\pm} \to 1, \quad \Phi_0 \to 0 \quad \text{as } Z \to \infty. \tag{4.27a,b}$$

Furthermore, the generic outer expansion (3.1) suggests that

$$C_1^{\pm}, \quad \Phi_1 \to 0 \quad \text{as } Z \to \infty. \tag{4.28}$$

Evidently, this expansion allows for non-zero limits of the $O(\delta^2)$ inner fields; using the $O(\delta^2)$ outer electro-neutrality (3.7) then yields

$$C_2^{\pm} \to c_2^{(s)}, \quad \Phi_2 \to \varphi_2^{(s)} \quad \text{as } Z \to \infty, \tag{4.29a,b}$$

where the superscript '(s)' indicates evaluation on s. Finally, since the outer pressure is $O(1)$,

$$P_{-2}, P_{-1} \to 0 \quad \text{as } Z \to \infty, \tag{4.30}$$

while

$$P_0 \to p_0^{(s)} \quad \text{as } Z \to \infty. \tag{4.31}$$

5. Inner analysis

5.1. *Leading-order inner analysis*

At leading $O(\delta^{-2})$ the ionic transport balances (4.9) yield $\partial J_{Z,-1}^{\pm}/\partial Z = 0$. Given the no-flux condition (4.18), we obtain vanishing of $O(\delta^{-1})$ ionic fluxes,

$$J_{Z,-1}^{\pm} \equiv 0. \tag{5.1}$$

https://doi.org/10.1017/jfm.2012.221 Published online by Cambridge University Press

Use of (4.26) then implies

$$\frac{\partial C_0^{\pm}}{\partial Z} \pm C_0^{\pm}\frac{\partial \Phi_0}{\partial Z} = 0. \tag{5.2}$$

Integration in conjunction with the large-Z matching condition (4.27) furnishes the Boltzmann distributions

$$C_0^{\pm} = \mathrm{e}^{\mp \Phi_0}, \tag{5.3}$$

or equivalently

$$C_0 = \cosh \Phi_0, \quad Q_0 = -\sinh \Phi_0. \tag{5.4}$$

For future reference, we note that addition of (5.2) yields a nil $O(\delta^{-1})$ salt flux,

$$\frac{\partial C_0}{\partial Z} + Q_0\frac{\partial \Phi_0}{\partial Z} = 0. \tag{5.5}$$

Substitution of (5.4) into the leading-order Poisson equation (4.12) yields the nonlinear Poisson–Boltzmann equation

$$\frac{\partial^2 \Phi_0}{\partial Z^2} = \sinh \Phi_0, \tag{5.6}$$

which is to be solved subject to the leading-order Gauss condition (cf. (4.19))

$$\frac{\partial \Phi_0}{\partial Z} = -\sigma \tag{5.7}$$

and (4.27*b*). A single integration in conjunction with the latter yields

$$\frac{\partial \Phi_0}{\partial Z} = -2\sinh\frac{\Phi_0}{2}; \tag{5.8}$$

another integration yields the Gouy–Chapman distribution

$$\tanh\frac{\Phi_0}{4} = \mathrm{e}^{-Z}\tanh\frac{\zeta}{4}, \tag{5.9}$$

in which

$$\zeta = \Phi_0(Z = 0). \tag{5.10}$$

Equations (5.7)–(5.8) provide the one-to-one correspondence between ζ and σ

$$\sigma = 2\sinh\frac{\zeta}{2}. \tag{5.11}$$

At $O(\delta^{-3})$, the momentum balance equation (4.13) in the z-direction reads

$$\frac{\partial P_{-2}}{\partial Z} + \frac{\alpha}{Pe}Q_0\frac{\partial \Phi_0}{\partial Z} = 0. \tag{5.12}$$

Use of the salt balance equation (5.5) and the matching conditions (4.27*a*) and (4.30) yields the osmotic pressure

$$P_{-2} = \frac{\alpha}{Pe}(C_0 - 1). \tag{5.13}$$

It is then readily verified that

$$\frac{\partial P_{-2}}{\partial X} + \frac{\alpha}{Pe}Q_0\frac{\partial \Phi_0}{\partial X} = 0, \tag{5.14}$$

https://doi.org/10.1017/jfm.2012.221 Published online by Cambridge University Press

so the momentum balance equation (4.14) in the x-direction is trivially satisfied at leading order.

5.2. *Second round*

With the Boltzmann distribution (5.3), both $J_X^{\pm}$ and $J_Y^{\pm}$ vanish at leading order, so the Nernst–Planck balances (4.9) at $O(\delta^{-1})$ yield $\partial J_{Z,0}^{\pm}/\partial Z = 0$. Use of the no-flux condition (4.18) then establishes the vanishing of the $O(1)$ ionic fluxes as well:

$$J_{Z,0}^{\pm} \equiv 0. \tag{5.15}$$

Asymptotic matching yields zero current and salt flux on s at $O(1)$, in agreement with the leading-order outer expressions (3.2)–(3.4).

Using (4.26), (5.15) becomes

$$\frac{\partial C_1^{\pm}}{\partial Z} \pm C_1^{\pm}\frac{\partial \Phi_0}{\partial Z} \pm C_0^{\pm}\frac{\partial \Phi_1}{\partial Z} = 0. \tag{5.16}$$

These are viewed as first-order differential equations governing $C_1^{\pm}$ in terms of the (yet unknown) potential Φ_1. These equations are subject to the decay condition (4.28); straightforward integration yields

$$C_1^{\pm} = \mp \Phi_1 \mathrm{e}^{\mp \Phi_0} \tag{5.17}$$

or

$$C_1 = \Phi_1 \sinh \Phi_0, \quad Q_1 = -\Phi_1 \cosh \Phi_0. \tag{5.18a,b}$$

We note that the vanishing of the $O(1)$ salt flux, obtained by addition of (5.16), reads

$$\frac{\partial C_1}{\partial Z} + Q_1\frac{\partial \Phi_0}{\partial Z} + Q_0\frac{\partial \Phi_1}{\partial Z} = 0. \tag{5.19}$$

The problem governing Φ_1 is discussed in the Appendix.

At $O(\delta^{-2})$, the momentum balance equation (4.13) in the z-direction is

$$\frac{\partial P_{-1}}{\partial Z} + \frac{\alpha}{Pe}\left(Q_1\frac{\partial \Phi_0}{\partial Z} + Q_0\frac{\partial \Phi_1}{\partial Z}\right) = 0. \tag{5.20}$$

Use of the nil salt flux (5.19) and the matching conditions (4.28) and (4.30) yields

$$P_{-1} = \frac{\alpha}{Pe}C_1. \tag{5.21}$$

It is then readily verified that

$$\frac{\partial P_{-1}}{\partial X} + \frac{\alpha}{Pe}\left(Q_1\frac{\partial \Phi_0}{\partial X} + Q_0\frac{\partial \Phi_1}{\partial X}\right) = 0, \tag{5.22}$$

and thus at $O(\delta^{-1})$ the momentum balance equation (4.14) in the x-direction yields

$$\frac{\partial^2 U_1}{\partial Z^2} = 0. \tag{5.23}$$

Two successive integrations, in conjunction with the no-slip condition (4.18) and a 2–1 Van Dyke matching procedure, yield

$$U_1 = \left(\frac{\partial u_0}{\partial z}\right)^{(s)} Z, \tag{5.24}$$

https://doi.org/10.1017/jfm.2012.221 Published online by Cambridge University Press

and similarly in the y-direction

$$V_1 = \left(\frac{\partial v_0}{\partial z}\right)^{(s)} Z. \tag{5.25}$$

Consider now the continuity equation (4.15). Use of the transformations (4.2) yields at $O(1)$

$$\frac{\partial U_1}{\partial \xi} + \frac{\partial V_1}{\partial \eta} + \frac{\partial W_2}{\partial Z} = 0. \tag{5.26}$$

Substitutions of the shear flows (5.24)–(5.25) followed by integration yields, in view of (4.16),

$$W_2 = -\frac{Z^2}{2}\left\{\frac{\partial}{\partial \xi}\left(\frac{\partial u_0}{\partial z}\right)^{(s)} + \frac{\partial}{\partial \eta}\left(\frac{\partial v_0}{\partial z}\right)^{(s)}\right\}. \tag{5.27}$$

Noting that differentiations with respect to ξ and η commute with evaluation at s and using the outer $O(1)$ continuity equation yields

$$W_2 = \frac{Z^2}{2}\left(\frac{\partial^2 w_0}{\partial z^2}\right)^{(s)}, \tag{5.28}$$

which automatically satisfies a 3–2 Van Dyke matching with the outer flow.

In view of the effective no-slip condition (3.6), $\partial u_0/\partial x = \partial v_0/\partial y = 0$ on s, whereby the leading-order outer continuity equation implies that $\partial w_0/\partial z$ vanishes there too. Use of (4.3) written in terms of the outer variables then shows that $\partial^2 w_0/\partial x^2 + \partial^2 w_0/\partial y^2 = 0$ on s as well; the outer momentum balance equation (3.5*b*) in the z-direction then yields $\partial^2 w_0/\partial z^2 = \partial p_0/\partial z$ on s. Thus, (5.28) reduces to

$$W_2 = \frac{Z^2}{2}\left(\frac{\partial p_0}{\partial z}\right)^{(s)}. \tag{5.29}$$

5.3. *Third round*

With the Boltzmann distributions (5.3) and (5.17), both $J_X^{\pm}$ and $J_Y^{\pm}$ also vanish at $O(\delta)$, so the Nernst–Planck equations (4.9) at $O(1)$ yield

$$\frac{\partial J_{Z,1}^{\pm}}{\partial Z} = 0. \tag{5.30}$$

These, together with the no-flux conditions (4.18), yield

$$J_{Z,1}^{\pm} \equiv 0. \tag{5.31}$$

Asymptotic matching then implies zero current and salt flux on s at $O(\delta)$, in agreement with the generic outer expansion (3.2)–(3.4).

Using (4.26), the nil ionic fluxes at $O(\delta)$ read

$$\frac{\partial C_2^{\pm}}{\partial Z} \pm C_2^{\pm}\frac{\partial \Phi_0}{\partial Z} \pm C_1^{\pm}\frac{\partial \Phi_1}{\partial Z} \pm C_0^{\pm}\frac{\partial \Phi_2}{\partial Z} = 0. \tag{5.32}$$

These are first-order differential equations governing $C_2^{\pm}$ in terms of the (yet unknown) potentials Φ_1 and Φ_2, which are subject to the matching condition (4.29). Integration yields here

$$C_2^{\pm} = \{c_2^{(s)} \mp (\Phi_2 - \varphi_2^{(s)}) + \tfrac{1}{2}\Phi_1^2\}\mathrm{e}^{\mp\Phi_0}, \tag{5.33}$$

https://doi.org/10.1017/jfm.2012.221 Published online by Cambridge University Press

or equivalently

$$C_2 = c_2^{(s)} \cosh \Phi_0 + (\Phi_2 - \varphi_2^{(s)}) \sinh \Phi_0 + \tfrac{1}{2}\Phi_1^2 \cosh \Phi_0,$$
$$Q_2 = -c_2^{(s)} \sinh \Phi_0 - (\Phi_2 - \varphi_2^{(s)}) \cosh \Phi_0 - \tfrac{1}{2}\Phi_1^2 \sinh \Phi_0. \tag{5.34}$$

For future reference we note that addition of (5.16) yields

$$\frac{\partial C_2}{\partial Z} + Q_2 \frac{\partial \Phi_0}{\partial Z} + Q_1 \frac{\partial \Phi_1}{\partial Z} + Q_0 \frac{\partial \Phi_2}{\partial Z} = 0, \tag{5.35}$$

representing nil salt flux at $O(\delta)$.

At $O(\delta^{-1})$, the momentum balance equation (4.13) in the z-direction reads

$$\frac{\partial P_0}{\partial Z} + \frac{\alpha}{Pe}\left(Q_2 \frac{\partial \Phi_0}{\partial Z} + Q_1 \frac{\partial \Phi_1}{\partial Z} + Q_0 \frac{\partial \Phi_2}{\partial Z}\right) = 0. \tag{5.36}$$

Using the salt balance equation (5.35) and the matching conditions (4.29*a*) and (4.31) provides the pressure

$$P_0 = p_0^{(s)} + \frac{\alpha}{Pe}\left(C_2 - c_2^{(s)}\right). \tag{5.37}$$

6. Effective slip condition

Consider now the $O(1)$ balance of the Stokes equation (4.14). Making use of the transformations (4.2)–(4.3) yields

$$\frac{\partial P_0}{\partial \xi} + \frac{\alpha}{Pe}\left(Q_2 \frac{\partial \Phi_0}{\partial \xi} + Q_1 \frac{\partial \Phi_1}{\partial \xi} + Q_0 \frac{\partial \Phi_2}{\partial \xi}\right) = \frac{\partial^2 U_2}{\partial Z^2} + (\boldsymbol{\nabla} \cdot \hat{\boldsymbol{n}}) \frac{\partial U_1}{\partial Z}. \tag{6.1}$$

At this stage, it is convenient to proceed assuming uniform surface charge, where ζ is uniform as well: see (5.11). Then, Φ_0 and hence also $C_0^{\pm}$ are functions of Z alone, independent of ξ and η. Substitution of (5.24), (5.37) and (5.34), and making use of the charge distributions (5.4) and (5.18), and (5.34) yields

$$\frac{\partial p_0^{(s)}}{\partial \xi} + \frac{\alpha}{Pe}\left\{(\cosh \Phi_0 - 1)\frac{\partial c_2^{(s)}}{\partial \xi} - \sinh \Phi_0 \frac{\partial \varphi_2^{(s)}}{\partial \xi}\right\} = \frac{\partial^2 U_2}{\partial Z^2} + (\boldsymbol{\nabla} \cdot \hat{\boldsymbol{n}})\left(\frac{\partial u_0}{\partial z}\right)^{(s)}. \tag{6.2}$$

Use of (5.6)–(5.8) allows for a single integration

$$\frac{\partial U_2}{\partial Z} = Z\left\{\frac{\partial p_0^{(s)}}{\partial \xi} - (\boldsymbol{\nabla} \cdot \hat{\boldsymbol{n}})\left(\frac{\partial u_0}{\partial z}\right)^{(s)}\right\}$$
$$+ \frac{\alpha}{Pe}\left\{2\left(1 - \cosh \frac{\Phi_0}{2}\right)\frac{\partial c_2^{(s)}}{\partial \xi} - \frac{\mathrm{d}\Phi_0}{\mathrm{d}Z}\frac{\partial \varphi_2^{(s)}}{\partial \xi}\right\} + M(\xi, \eta), \tag{6.3}$$

https://doi.org/10.1017/jfm.2012.221 Published online by Cambridge University Press

wherein M is an 'integration constant'. Using again (5.8) allows for yet another integration, where accounting for the no-slip condition (4.17) yields

$$U_2 = \frac{Z^2}{2}\left\{\frac{\partial p_0^{(s)}}{\partial \xi} - (\boldsymbol{\nabla}\cdot\hat{\boldsymbol{n}})\left(\frac{\partial u_0}{\partial z}\right)^{(s)}\right\} + \frac{\alpha}{Pe}\left\{4\ln\frac{\cosh(\Phi_0/4)}{\cosh(\zeta/4)}\frac{\partial c_2^{(s)}}{\partial \xi} + (\zeta-\Phi_0)\frac{\partial \varphi_2^{(s)}}{\partial \xi}\right\} + M(\xi,\eta)Z. \tag{6.4}$$

Performing a 3–2 Van Dyke matching procedure, we find that $M = 0$ and

$$u_2^{(s)} = \frac{\alpha}{Pe}\left\{\zeta\frac{\partial \varphi_2^{(s)}}{\partial \xi} - \mathscr{H}(\zeta)\frac{\partial c_2^{(s)}}{\partial \xi}\right\}. \tag{6.5}$$

Here,

$$\mathscr{H}(\zeta) = -2\ln\left(1-\tanh^2\frac{\zeta}{4}\right). \tag{6.6}$$

In addition, the matching procedure also requires that

$$\frac{\partial p_0^{(s)}}{\partial \xi} - (\boldsymbol{\nabla}\cdot\hat{\boldsymbol{n}})\left(\frac{\partial u_0}{\partial z}\right)^{(s)} = \left(\frac{\partial^2 u_0}{\partial z^2}\right)^{(s)}, \tag{6.7}$$

which, however, is automatically satisfied in view of the outer Stokes equation and relation (4.3) written for u_0 in terms of the unstrained Cartesian coordinates.

The analysis of momentum balance in the y-direction furnishes an expression similar to (6.5) for $v_2^{(s)}$. Moreover, an asymptotic 3–2 Van Dyke matching procedure reveals that $w_2^{(s)} = 0$. In invariant notation, we find the macroscale slip condition

$$\boldsymbol{v}_2^{(s)} = \frac{\alpha}{Pe}\left\{\zeta\boldsymbol{\nabla}_s\varphi_2 - \mathscr{H}(\zeta)\boldsymbol{\nabla}_s c_2\right\}, \tag{6.8}$$

wherein $\boldsymbol{\nabla}_s = (\boldsymbol{I}-\hat{\boldsymbol{n}}\hat{\boldsymbol{n}})\cdot\boldsymbol{\nabla}$ is the surface-gradient operator.

7. Inhomogeneous Neumann conditions

We finally consider the Nernst–Planck equations (4.9) at $O(\delta)$. With uniform zeta, $C_0^{\pm}$ are independent of ξ and η, resulting in

$$\frac{\partial J_{Z,2}^{\pm}}{\partial Z} + Pe\,W_2\frac{\partial C_0^{\pm}}{\partial Z} = 0. \tag{7.1}$$

This is the first asymptotic order in which advection terms appear, leading to non-zero ionic fluxes in the z-direction. (Due to the dependence (5.33) of $C_2^{\pm}$ on $c_2^{(s)}$ and $\varphi_2^{(s)}$, the tangential fluxes $J_{X,2}^{\pm}$ and $J_{Y,2}^{\pm}$ are in general non-zero and seemingly should contribute to the above balance. The dependence of these fluxes on tangential coordinates, however, occurs through the coordinates ξ and η. Applying the transformation (4.2), we see that the contribution of these fluxes will actually appear at the next $O(\delta^2)$ level of (4.9).)

Substitution of (5.29) yields

$$J_{Z,2}^{\pm} = Pe\left(\frac{\partial p_0}{\partial z}\right)^{(s)}\left\{\int_0^Z Z' C_0^{\pm}\,\mathrm{d}Z' - \frac{Z^2}{2}C_0^{\pm}\right\}. \tag{7.2}$$

https://doi.org/10.1017/jfm.2012.221 Published online by Cambridge University Press

Carefully performing the limit $Z \to \infty$ then provides the fluxes

$$J^{\pm}_{Z,2}(Z \to \infty) = Pe\left(\frac{\partial p_0}{\partial z}\right)^{(s)} \int_0^{\infty} Z(C_0^{\pm} - 1)\,\mathrm{d}Z. \tag{7.3}$$

Addition of both expressions (7.3) in conjunction with (5.3) yields the $O(\delta^2)$ salt flux

$$Pe\left(\frac{\partial p_0}{\partial z}\right)^{(s)} \int_0^{\infty} Z(\cosh \Phi_0 - 1)\,\mathrm{d}Z; \tag{7.4}$$

integration by parts in conjunction with (5.8) reveals that the integral is $\mathscr{H}(\zeta)$. Similarly, subtraction of both expressions yields the $O(\delta^2)$ current density

$$-Pe\left(\frac{\partial p_0}{\partial z}\right)^{(s)} \int_0^{\infty} Z \sinh \Phi_0\,\mathrm{d}Z; \tag{7.5}$$

here integration by parts reveals that the integral is ζ.

Asymptotic matching with the outer expressions (3.8) readily provides an inhomogeneous Neumann condition governing the $O(\delta^2)$ outer salt perturbation and electric potential. In invariant notation,

$$\frac{\partial c_2}{\partial n} = -\mathscr{H}(\zeta)\, Pe \frac{\partial p_0}{\partial n}, \quad \frac{\partial \varphi_2}{\partial n} = \zeta\, Pe \frac{\partial p_0}{\partial n}. \tag{7.6a,b}$$

The successful matching with the outer variables, in both § 6 and the present section, justifies *a posteriori* the postulated generic expansion (3.1) in the outer region.

8. Extension to unsteady problems

The preceding analysis was carried out in a reference frame attached to the solid wall, assuming steady-state transport. In the general case, however, such a reference frame may not exist. For example, in the problem of a particle approaching a charged wall, there is no reference frame in which both surfaces are stationary; in that problem, moreover, the transport is unsteady in all frames of reference. Here we extend our analysis to the general case.

For unsteady transport, the Nernst–Planck equations (2.7) become

$$\boldsymbol{\nabla} \cdot \boldsymbol{j}^{\pm} + Pe\left(\frac{\partial c^{\pm}}{\partial t} + \boldsymbol{v} \cdot \boldsymbol{\nabla} c^{\pm}\right) = 0, \tag{8.1}$$

where the time t is normalized by a^*/v^*. The no-slip condition (2.19) now reads

$$\boldsymbol{v} = \boldsymbol{v}_S \quad \text{on } S, \tag{8.2}$$

wherein the surface velocity distribution $\boldsymbol{v}_S$ corresponds to a rigid-body motion with angular velocity $\boldsymbol{\Omega}$. The Stokes flow is still quasi-steady, its time-dependence being introduced by the varying geometry associated with the rigid-body motion of the solid surfaces.

The outer analysis of § 3 remains unchanged, except for (3.9) governing the salt perturbation, now reading

$$\nabla^2 c_2 = Pe\left(\frac{\partial c_2}{\partial t} + \boldsymbol{v}_0 \cdot \boldsymbol{\nabla} c_2\right). \tag{8.3}$$

https://doi.org/10.1017/jfm.2012.221 Published online by Cambridge University Press

In the inner domain, the wall-fixed Cartesian system (x, y, z) now rotates with the solid-wall angular velocity $\boldsymbol{\Omega}$. It is useful to re-define the inner velocity through

$$\boldsymbol{v} = \boldsymbol{v}_S(\mathscr{P}) + \boldsymbol{\Omega} \times \boldsymbol{r} + \boldsymbol{V}. \tag{8.4}$$

Here, $\boldsymbol{r} = (x, y, z)$ is the relative position vector and $\boldsymbol{V}$, the velocity field observed within the rotating frame (x, y, z), possesses the same scaling as in (4.4)–(4.5), namely

$$\boldsymbol{V} = (\delta U, \delta V, \delta^2 W). \tag{8.5}$$

With this definition (4.16)–(4.18) remain valid. We define $\partial/\partial T$ as the partial time derivative in the rotating frame of reference (i.e. with x, y, and z fixed),

$$\frac{\partial}{\partial T} = \frac{\partial}{\partial t} + (\boldsymbol{v}_S + \boldsymbol{\Omega} \times \boldsymbol{r}) \cdot \boldsymbol{\nabla}. \tag{8.6}$$

The unsteady Nernst–Planck equations (4.9) then read

$$\delta^{-2}\frac{\partial J_Z^{\pm}}{\partial Z} + \delta^{-1}\left(\frac{\partial J_X^{\pm}}{\partial X} + \frac{\partial J_Y^{\pm}}{\partial Y}\right) + Pe\frac{\partial C^{\pm}}{\partial T} + \delta\, Pe\left(\delta^{-1/2}U\frac{\partial C^{\pm}}{\partial X} + \delta^{-1/2}V\frac{\partial C^{\pm}}{\partial Y} + W\frac{\partial C^{\pm}}{\partial Z}\right) = 0. \tag{8.7}$$

Evidently, the analysis of these equations at $O(\delta^{-2})$ and $O(\delta^{-1})$ is unaffected by the unsteadiness embodied in the third term. It may appear as though (8.7) would be modified at $O(1)$ and $O(\delta)$ by the terms $\partial C_0^{\pm}/\partial T$ and $\partial C_1^{\pm}/\partial T$, respectively. However, the analysis of the Nernst–Planck equations at orders δ^{-2} and δ^{-1} (see § 5) provides equilibrium distributions for both $C_0^{\pm}$ and $C_1^{\pm}$ in terms of Φ_0 and Φ_1. The leading-order potential Φ_0 is uniquely determined by the zeta potential distribution: see (5.9). This applies to Φ_1 as well (see Appendix). Accordingly, the above time derivatives vanish. The inner analysis of §§ 5–7 is therefore unaffected by the unsteadiness, whereby the slip condition (6.8) and Neumann conditions (7.6) remain valid.

9. Recapitulation of the macroscale model

Here we outline the macroscale scheme for solving a generic flow-driven electrokinetic problem within the electro-neutral bulk, where the generic asymptotic expansion (3.1) holds.

(*a*) First, the leading-order driving flow $(\boldsymbol{v}_0, p_0)$ needs to be calculated. It is governed by the continuity and homogeneous Stokes equations (3.5), the effective no-slip boundary condition $\boldsymbol{v}_0 = \boldsymbol{v}_S$ (see (8.2)), and a prescribed Stokes flow at large distances away from the particle

$$\boldsymbol{v}_0 \sim \boldsymbol{v}_\infty(\boldsymbol{x}) \quad \text{as } |\boldsymbol{x}| \to \infty. \tag{9.1}$$

(*b*) The streaming-potential φ_2 and salt concentration perturbation c_2 are then calculated. The former is governed by Laplace's equation (3.10), an attenuation condition far away from the particle (see (2.25)), and the inhomogeneous Neumann boundary condition

$$\frac{\partial \varphi_2}{\partial n} = \zeta\, Pe\frac{\partial p_0}{\partial n} \quad \text{on } s; \tag{9.2}$$

https://doi.org/10.1017/jfm.2012.221 Published online by Cambridge University Press

the latter is governed by the advection–diffusion equation

$$\nabla^2 c_2 = Pe\left(\frac{\partial c_2}{\partial t} + \boldsymbol{v}_0 \cdot \nabla c_2\right), \tag{9.3}$$

the attenuation condition (2.24*a*), and the inhomogeneous Neumann condition

$$\frac{\partial c_2}{\partial n} = -\mathscr{H}(\zeta)\, Pe \frac{\partial p_0}{\partial n} \quad \text{on } s, \tag{9.4}$$

wherein $\mathscr{H}(\zeta)$ is defined in (6.6).

(*c*) The flow correction $(\boldsymbol{v}_2, p_2)$ is governed by the homogeneous Stokes equations (3.11), the attenuation requirement at infinity, and the slip condition

$$\boldsymbol{v}_2 = \frac{\alpha}{Pe}\{\zeta \nabla_s \varphi_2 - \mathscr{H}(\zeta)\nabla_s c_2\} \quad \text{on } s. \tag{9.5}$$

A typical flow-driven electrokinetic problem concerns one or more particles suspended in an electrolyte solution and subject to a prescribed flow. In choosing the arbitrary surface over which the quadratures (2.27) and (2.30) are evaluated, it is convenient to employ the outer edge s of the Debye layer where the outer expansions (3.1) apply. This leads to the expansion

$$\boldsymbol{F} = \boldsymbol{F}_0 + \delta^2 \boldsymbol{F}_2 + \cdots \tag{9.6}$$

and a similar one for $\boldsymbol{T}$. Here,

$$\boldsymbol{F}_0 = \oint_S \mathrm{d}A\, \hat{\boldsymbol{n}} \cdot \boldsymbol{N}_0, \quad \boldsymbol{T}_0 = \oint_S \mathrm{d}A\, (\boldsymbol{x} - \boldsymbol{x}_0) \times \left(\hat{\boldsymbol{n}} \cdot \boldsymbol{N}_0\right) \tag{9.7a,b}$$

are the zeroth-order force and torque, with

$$\boldsymbol{N}_0 = -p_0 \boldsymbol{I} + (\nabla \boldsymbol{v}_0) + (\nabla \boldsymbol{v}_0)^{\mathrm{T}}. \tag{9.8}$$

Clearly, these force and torque represent the hydrodynamic loads in the absence of electrokinetic effects. Our interest lies in analysing the effects of electro-viscous forces on particle motion. Thus we need to calculate the corrections

$$\boldsymbol{F}_2 = \oint_S \mathrm{d}A\, \hat{\boldsymbol{n}} \cdot \boldsymbol{N}_2, \quad \boldsymbol{T}_2 = \oint_S \mathrm{d}A\, (\boldsymbol{x} - \boldsymbol{x}_0) \times \left(\hat{\boldsymbol{n}} \cdot \boldsymbol{N}_2\right), \tag{9.9a,b}$$

where

$$\boldsymbol{N}_2 = -p_2 \boldsymbol{I} + (\nabla \boldsymbol{v}_2) + (\nabla \boldsymbol{v}_2)^{\mathrm{T}} \tag{9.10}$$

is the Newtonian stress corresponding to the induced flow perturbation. Note that (contrary to the large-Pe limit, part 1) the contribution of Maxwell stresses enters only at $O(\delta^4)$.

Evidently, calculation of the electro-viscous force correction entails in general the evaluation of two asymptotic orders of the flow variables as well as the leading-order calculation of the electric field and salt perturbation. These terms are provided by the calculation procedure summarized above.

Following Brenner (1964), the electro-viscous force (and torque) on the particle (9.9) may be evaluated directly from (9.5) by use of the Lorentz reciprocal theorem for Stokes flows (Happel & Brenner 1965) without actually solving for the perturbation $\boldsymbol{v}_2$.

https://doi.org/10.1017/jfm.2012.221 Published online by Cambridge University Press

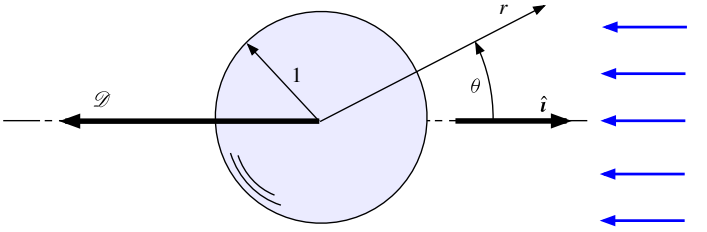


FIGURE 2. (Colour online available at journals.cambridge.org/flm) Schematic of the translating sphere problem. In the particle-fixed reference frame the fluid at infinity streams at a unit velocity in the $-\hat{\boldsymbol{\imath}}$-direction.

Note that in the context of a mobility problem, the electro-viscous force and torque result in excess particle linear and angular velocities of $O(\delta^2)$, not accounted for in (9.5). However, as the flow problem at $O(\delta^2)$ is linear, corrections to the particle velocities can be calculated, if desired, using mobility relations which are in principle known from the zeroth-order flow solution.

Our macroscale paradigm is illustrated in the next section for the prototype problem of sphere sedimentation.

10. Illustration: the excess drag on a translating particle

Consider a spherical particle (radius a^*) translating with a constant speed v^* in an otherwise quiescent unbounded fluid. The direction of the particle velocity is defined by the unit vector $\hat{\boldsymbol{\imath}}$. In standard Stokes flows (i.e. in the absence of electrokinetic effects) the drag on the particle (the hydrodynamic force in the $-\hat{\boldsymbol{\imath}}$-direction) is $\mathscr{D}^* = 6\pi\mu a^* v^*$. Our goal is to calculate the electro-viscous correction to this formula.

We employ the moderate-Péclet-number macroscale model as summarized in the previous section. We analyse the problem in a particle-fixed reference frame, where the transport is steady. Thus, $\boldsymbol{v}_\infty = -\hat{\boldsymbol{\imath}}$ and $\boldsymbol{v}_S = \boldsymbol{0}$. It is convenient to use spherical coordinates (r, θ), $r = 0$ at the particle centre and $\theta = 0$ in the $\hat{\boldsymbol{\imath}}$-direction. The particle boundary is then $r = 1$ while the fluid velocity vector adopts the form $\boldsymbol{v} = \hat{\boldsymbol{e}}_r u + \hat{\boldsymbol{e}}_\theta v$. Figure 2 defines the geometric configuration of the problem.

The (hydrodynamic and electric) drag on the particle is $\mathscr{D} = -\hat{\boldsymbol{\imath}} \cdot \boldsymbol{F}$. The driving field $(\boldsymbol{v}_0, p_0)$, corresponding to the flow in the absence of electrokinetic effects, is well known (Happel & Brenner 1965):

$$u_0 = -\left(1 - \frac{3}{2r} + \frac{1}{2r^3}\right)\cos\theta, \quad v_0 = \left(1 - \frac{3}{4r} - \frac{1}{4r^3}\right)\sin\theta, \quad p_0 = \frac{3}{2r^2}\cos\theta. \tag{10.1a,b,c}$$

For this flow $\mathscr{D}_0 = 6\pi$. The electro-viscous drag correction $\mathscr{D}_2$ is calculated by integrating the viscous stresses corresponding to the flow perturbation $\boldsymbol{v}_2$ over the particle surface: see (9.9*a*). This flow depends, through the linear combination in the effective slip condition (9.5), on both the streaming potential φ_2 and the salt-concentration perturbation c_2. We consider each term separately.

The calculation of the electro-osmotic contribution is straightforward. Since both φ_2 and p_2 are harmonic and decay at infinity, (9.2) readily yields (Bike & Prieve 1992; Yariv *et al.* 2011)

$$\varphi_2 \equiv \zeta\, Pe\, p_0. \tag{10.2}$$

https://doi.org/10.1017/jfm.2012.221 Published online by Cambridge University Press

The electro-osmotic slip term then reads $\boldsymbol{v}_{2,E} = \alpha\zeta^2\boldsymbol{\nabla}_s p_0$. The contribution $\mathscr{D}_{2,E}$ to the drag correction corresponding to this slip distribution is readily calculated (see a similar calculation in part 1):

$$\mathscr{D}_{2,E} = 6\pi\alpha\zeta^2. \tag{10.3}$$

The diffuso-osmotic contribution is more difficult to handle. Defining

$$c_2 = \mathscr{H}(\zeta)\, Pe\, \tilde{c}, \tag{10.4}$$

we find that the reduced concentration $\tilde{c}$ is governed by the advection–diffusion equation (cf. (9.3))

$$\nabla^2\tilde{c} = Pe\, \boldsymbol{v}_0 \cdot \boldsymbol{\nabla}\tilde{c}, \tag{10.5}$$

together with the Neumann condition (cf. (9.4))

$$\frac{\partial\tilde{c}}{\partial r} = -\frac{\partial p_0}{\partial r} \quad \text{at } r = 1 \tag{10.6}$$

and the requirement of decay at infinity. The concentration $\tilde{c}$ is thus independent of ζ. The diffuso-osmotic slip associated with $\tilde{c}$ is

$$\boldsymbol{v}_{2,D} = -\alpha\mathscr{H}^2(\zeta)\boldsymbol{\nabla}_s\tilde{c}. \tag{10.7}$$

A closed-form solution of equation (10.5) is not available. We first consider the respective limits of small and large Pe numbers, and then present a semi-analytic solution for arbitrary Pe.

10.1. *Small-Pe solution*

When Pe is small we find at leading order a relation similar to (10.2), namely

$$\tilde{c} = -p_0. \tag{10.8}$$

The associated drag contribution is therefore (cf. (10.3))

$$\mathscr{D}_{2,D} = 6\pi\alpha\mathscr{H}^2(\zeta), \tag{10.9}$$

and the total drag correction is

$$\mathscr{D}_2 = 6\pi\alpha\left(\zeta^2 + \mathscr{H}^2(\zeta)\right). \tag{10.10}$$

This is actually the expression obtained by Cox (1997) in his small-Pe analysis.

10.2. *Large-Pe solution*

The large-Pe limit is singular. Naïvely, the dominant advection in (10.5) in conjunction with a pattern consisting of open streamlines originating at infinity (where $\tilde{c}$ vanishes) imply $\tilde{c} \equiv 0$. This solution is however incompatible with (10.6). A boundary layer wherein $\tilde{c}$ is non-zero therefore develops in the vicinity of $r = 1$. The thickness of this layer $\Delta \ll 1$ is determined by the balance between diffusion and advection in (10.5). Since the velocity field $\boldsymbol{v}_0$ satisfies effective no-slip conditions at $r = 1$ (see (8.2)) and varies on the particle scale, its radial and tangential components within the boundary layer are of orders Δ^2 and Δ, respectively. It then follows that $\Delta = Pe^{-1/3}$ (Leal 2007). Condition (10.6) then implies that $\tilde{c}$ is $O(Pe^{-1/3})$. We accordingly define the transverse boundary-layer coordinate and the scaled concentration

$$\Xi = Pe^{1/3}(r-1), \qquad \Gamma = Pe^{1/3}\tilde{c}. \tag{10.11a,b}$$

https://doi.org/10.1017/jfm.2012.221 Published online by Cambridge University Press

Using the boundary-layer approximation for the driving flow (10.1), we obtain from (10.5) the leading-order advection–diffusion equation governing $\Gamma(\Xi, \theta)$:

$$\frac{\partial^2 \Gamma}{\partial \Xi^2} = \frac{3}{2}\left(\Xi \sin\theta \frac{\partial \Gamma}{\partial \theta} - \Xi^2 \cos\theta \frac{\partial \Gamma}{\partial \Xi}\right) \quad \text{for } \Xi > 0. \tag{10.12}$$

This is supplemented by the boundary condition

$$\frac{\partial \Gamma}{\partial \Xi} = \frac{9}{2}\cos\theta \quad \text{at } \Xi = 0, \tag{10.13}$$

obtained via substitution of p_0 from (10.1*c*) into (10.6), together with the requirement of decay at large Ξ. The appearance of this boundary layer was discussed in part 1.

10.3. *Semi-analytic solution*

For arbitrary Pe, we employ a spectral expansion in Legendre polynomials

$$\tilde{c} = \sum_{n=0}^{\infty} c^{(n)}(r, Pe) P^{(n)}(\eta), \tag{10.14}$$

wherein $\eta = \cos\theta$ and $P^{(n)}$ is the Legendre polynomial of degree n. Substitution of (10.14) into (10.5)–(10.6) in conjunction with the orthogonality properties of the Legendre polynomials provides an infinite system of ordinary differential equations governing the coefficients $\{c^{(n)}\}$ together with appropriate boundary conditions. This system is truncated and integrated numerically (see e.g. Michelin & Lauga 2011).

The diffuso-osmotic slip is given by

$$\boldsymbol{v}_{2,D} = \hat{\boldsymbol{e}}_\theta \alpha \mathscr{H}^2(\zeta) \sum_{n=0}^{\infty} c^{(n)}(1, Pe) \frac{\mathrm{d}P^{(n)}}{\mathrm{d}\eta} \sin\theta. \tag{10.15}$$

This slip engenders a velocity field whose associated stress is denoted $\boldsymbol{N}_{2,D}$. The corresponding excess drag is

$$\mathscr{D}_{2,D} = -\oint_s \mathrm{d}A\, \hat{\boldsymbol{n}} \cdot \boldsymbol{N}_{2,D} \cdot \hat{\boldsymbol{\imath}}. \tag{10.16}$$

Following Brenner (1964), $\mathscr{D}_{2,D}$ is calculated via application of the reciprocal theorem. Thus,

$$\mathscr{D}_{2,D} = -\oint_s \mathrm{d}A\, \hat{\boldsymbol{n}} \cdot \boldsymbol{N}_T \cdot \boldsymbol{v}_{2,D}, \tag{10.17}$$

wherein $\boldsymbol{N}_T$ is the Newtonian stress field associated with translation of the particle with velocity $\hat{\boldsymbol{\imath}}$. For the Stokes flow (10.1) associated with translation in a unit velocity $\hat{\boldsymbol{n}} \cdot \boldsymbol{S}_T = -(3/2)\hat{\boldsymbol{\imath}}$ (Happel & Brenner 1965). Substitution of (10.15) and use of the orthogonality properties of the Legendre polynomials readily provides the diffuso-osmotic drag

$$\mathscr{D}_{2,D} = -4\pi\alpha \mathscr{H}^2(\zeta) c^{(1)}(1, Pe), \tag{10.18}$$

which only depends on the coefficient of the dipole mode $c^{(1)}$ in the expansion (10.14). The total drag correction is

$$\mathscr{D}_2 = 6\pi\alpha\zeta^2 - 4\pi\alpha \mathscr{H}^2(\zeta) c^{(1)}(1, Pe). \tag{10.19}$$

https://doi.org/10.1017/jfm.2012.221 Published online by Cambridge University Press

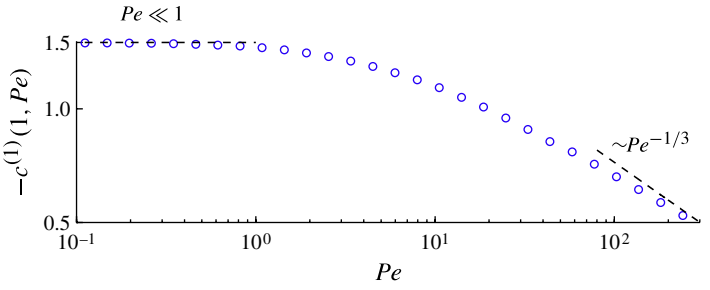


FIGURE 3. (Colour online) Variation of $-c^{(1)}(1, Pe)$ with Pe on a logarithmic scale. At large Pe the curve is asymptotic to a straight line with slope $-1/3$.

Figure 3 presents the variation of $-c^{(1)}(1, Pe)$ with Pe on a logarithmic scale. At small Pe the value $3/2$ is approached, in agreement with (10.8). The $Pe^{-1/3}$ scaling at large Pe is already visible at $Pe \approx 200$. With that scaling, the large-Pe excess drag is dominated by the electro-osmotic contribution (10.3). This is in agreement with the value calculated in part 1 for the same problem.

We emphasize, however, that quantities pertaining to the limit considered in part 1 – moderate Hartmann numbers, $\lambda \sim O(1)$ – cannot in general be recovered by applying the large-Pe limit to the present scheme: it cannot capture the contribution of Maxwell stresses, which appear at leading order in the former scheme. The coincidence between large-Pe excess drag in the present model and the excess drag in the moderate-λ problem has to do with the unboundedness of the fluid domain, where no excess drag is contributed by the Maxwell stresses (Yariv 2006).

The different role played by electro-osmosis and diffuso-osmosis, corresponding to the first and second terms in the excess drag (10.19), is related to the different equations governing the electric potential and salt concentration. While both satisfy similar Neumann conditions (see (9.2) and (9.4)), the differential equations are different: the salt concentration is affected by advection with the driving velocity field. The effect of advection is illustrated in figure 4, showing lines of constant c_2 for $Pe = 0$ and $Pe = 5$. The former also represent (for all Pe) equipotentials of φ_2.

11. Discussion

The present paper is a natural sequel to part 1, where a scaling relationship between the Péclet and Hartmann numbers was identified for generic flow-driven electrokinetic phenomena in the thin-double-layer limit. The linkage between these two parameters has apparently been overlooked in the pioneering analysis of Cox (1997). We have accordingly revisited the generic problem of flow-driven electrokinetic phenomena with the goal of deriving a macroscale model in the thin-double-layer limit. Whereas in part 1 we focused on large Péclet numbers, here we address the more challenging problem of moderate Péclet numbers, where bulk concentration gradients affect the leading-order electro-viscous forces.

As in part 1, the physics of the Debye-layer is embodied in the macroscale description through effective boundary conditions describing the generation of electric potential and salt polarization in the bulk. These originate from the non-uniform streaming currents within the Debye layer, associated with the driving flow. The potential and salt gradients animate (through electro-osmotic and diffuso-osmotic slip) an electrokinetic flow perturbation, in turn giving rise to electro-viscous forces. In

https://doi.org/10.1017/jfm.2012.221 Published online by Cambridge University Press

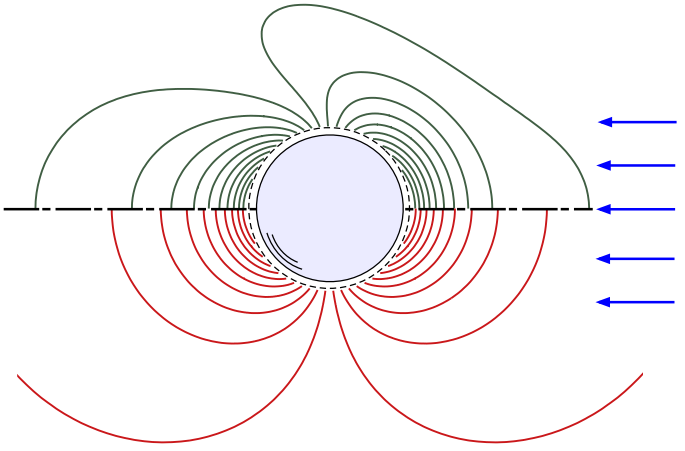


FIGURE 4. (Colour online) Lines of constant c_2 for $Pe = 0$ (bottom) and $Pe = 5$ (top). The fore–aft symmetric pattern at the bottom also represents the equipotentials of φ_2 (for all Pe).

contrast with the large-Péclet-number limit described in part 1, Maxwell stresses here do not affect the leading-order electro-viscous forces.

While the present scheme has formally been developed for moderate Péclet numbers, it actually applies to small Péclet numbers as well. At this limit the Hartmann number, which is $O(\delta^{-2})$ to begin with, is still larger. To understand the small-Pe limit, consider the Coulomb body force in the Stokes equations (2.11), $\lambda q \boldsymbol{\nabla}\varphi$. The conservative part of it is balanced by a comparable osmotic pressure term, carrying no dynamic effect. The non-conservative part, associated with the $O(\delta^2\, Pe)$ induced electric field (see (2.6)), is of order $\delta^2\, Pe\, \lambda\, q$. In the Debye layer, q is of order unity; in view of (2.4), so is then the non-conservative body force. The $O(\delta^2)$ induced electro-osmotic flow is therefore independent of Pe in that limit. Similar arguments reveal that the same also holds for the diffuso-osmotic slip. It is therefore established that small-Péclet-number limit is essentially non-singular. This explains why Cox (1997), while apparently unaware of the relationship between the Hartmann and Péclet numbers, obtained the correct electro-viscous drag correction in that limit.

Both the present derivation and that of part 1 present the usefulness of the singular thin double-layer limit, which allows derivations of macroscale models for arbitrary geometries without resorting to *ad hoc* approximations common in the literature. Thus, for instance, there is no restriction to small perturbations from equilibrium. This prevailing approximation, while useful in analysing electrokinetic transport for double layers that are not thin, is obscure in the thin double-layer limit. Here the imposed flow can hardly be considered a 'perturbation' in the bulk fluid domain, where the equilibrium fields are exponentially small. In the present context, where the Péclet number is moderate (and certainly in that of part 1), such an assumption is clearly inappropriate.

Our macroscale paradigm has been illustrated in the context of the prototype problem of particle sedimentation. The electro-viscous excess drag, above and beyond the familiar Stokes drag, is animated by both electro-osmotic and diffuso-osmotic slip. The contribution associated with the latter is a monotonically decreasing function of the Péclet number Pe: At small Pe it approaches a maximum value, independent of Pe;

https://doi.org/10.1017/jfm.2012.221 Published online by Cambridge University Press

at large Pe, where the salt perturbation adopts a boundary layer profile, it is $O(Pe^{-1/3})$ small.

The macroscale model yields an electro-viscous force which is nonlinear in the driving flow: while the electro-osmotic slip is linearly dependent on the animating flow, the diffuso-osmotic slip is nonlinear owing to the advection term in the equation governing the salt polarization. In the present illustration the nonlinearity is implicit in the dependence of the drag coefficient $\mathscr{D}_2$ on Pe. A different type of nonlinearity associated with Maxwell stresses occurs in part 1. Both nonlinearities can in general violate the familiar reversibility properties of Stokes flows. The irreversibility associated with the Maxwell stresses was demonstrated by Schnitzer, Khair & Yariv (2011). Irreversibilities associated with diffuso-osmotic slip will be discussed in a future contribution.

Since Péclet-number scaling larger than δ^{-2} is unlikely to be encountered in practice, we conclude that the schemes described in parts 1 and 2 essentially cover the entire spectrum of flow-driven electrokinetic phenomena.

Acknowledgements

This work was supported by a seed grant from the Russell Berrie Nanotechnology Institute. E.Y. was also supported by the Israel Science Foundation (grant no. 114/09).

Appendix. The problem governing Φ_1

The differential equation governing Φ_1 is obtained from $O(\delta)$ of (4.12) together with (4.3) and (5.18):

$$\frac{\partial^2 \Phi_1}{\partial Z^2} - \Phi_1 \cosh \Phi_0 = -\boldsymbol{\nabla} \cdot \hat{\boldsymbol{n}} \frac{\partial \Phi_0}{\partial Z}. \tag{A 1}$$

From (5.9),

$$\frac{\partial \Phi_0}{\partial Z} = -\frac{4A\mathrm{e}^{-Z}}{1 - A^2\mathrm{e}^{-2Z}}, \tag{A 2}$$

wherein $A = \tanh(\zeta/4)$. A particular integral of (A 1) satisfying the decay condition (4.28) is

$$-A\mathrm{e}^{-Z} \frac{2Z + A^2\mathrm{e}^{-2Z}}{1 - A^2\mathrm{e}^{-2Z}} \boldsymbol{\nabla} \cdot \hat{\boldsymbol{n}}. \tag{A 3}$$

One complementary solution of (A 1), which also decays at large Z, is

$$\frac{\mathrm{e}^{-Z}}{1 - A^2\mathrm{e}^{-2Z}}. \tag{A 4}$$

The other solution diverges at large Z and is therefore rejected. The integration constant (generally a function of ξ and η) multiplying (A 4) is determined by the $O(\delta)$ balance of Gauss's condition (4.19) at $Z = 0$,

$$\frac{\partial \Phi_1}{\partial Z} = \gamma \frac{\partial \bar{\varphi}_0}{\partial n}, \tag{A 5}$$

in which $\bar{\varphi}_0$ is the leading-order electric potential within the solid. This field, in turn, is governed by Laplace's equation together with the leading-order balance of (2.23), which, in view of (5.10), simply reads

$$\bar{\varphi}_0 = \zeta. \tag{A 6}$$

https://doi.org/10.1017/jfm.2012.221 Published online by Cambridge University Press

For a uniform surface charge density σ on S, where ζ is constant, $\bar{\varphi}_0 \equiv \zeta$ and (A 5) becomes homogeneous.

The detailed solution of Φ_1 is not required in calculating the leading-order electroviscous forces. It is nonetheless important to notice (see § 8) that Φ_1 is completely determined by the zeta-potential (or, equivalently, the surface-charge) distribution, and is accordingly independent of the imposed flow.

REFERENCES

ALEXANDER, B. M. & PRIEVE, D. C. 1987 A hydrodynamic technique for measurement of colloidal forces. *Langmuir* **3** (5), 788–795.

BIKE, S. G. & PRIEVE, D. C. 1990 Electrohydrodynamic lubrication with thin double layers. *J. Colloid Interface Sci.* **136** (1), 95–112.

BIKE, S. G. & PRIEVE, D. C. 1992 Electrohydrodynamics of thin double layers: a model for the streaming potential profile. *J. Colloid Interface Sci.* **154**, 87–96.

BOOTH, F. 1950 The cataphoresis of spherical, solid non-conducting particles in a symmetrical electrolyte. *Proc. R. Soc. Lond. Ser.* A. *Math. Phys. Sci.* **203** (1075), 514.

BOOTH, F. 1954 Sedimentation potential and velocity of solid spherical particles. *J. Chem. Phys.* **22**, 1956–1968.

BRENNER, H. 1964 The Stokes resistance of an arbitrary particle. Part 4. Arbitrary fields of flow. *Chem. Engng Sci.* **19**, 703–727.

COX, R. G. 1997 Electroviscous forces on a charged particle suspended in a flowing liquid. *J. Fluid Mech.* **338**, 1–34.

DUKHIN, S. S. 1993 Non-equilibrium electric surface phenomena. *Adv. Colloid Interface Sci.* **44**, 1–134.

HAPPEL, J. & BRENNER, H. 1965 *Low Reynolds Number Hydrodynamics*. Prentice-Hall.

KEH, H. J. & ANDERSON, J. L. 1985 Boundary effects on electrophoretic motion of colloidal spheres. *J. Fluid Mech.* **153**, 417–439.

LEAL, L. G. 2007 *Advanced Transport Phenomena: Fluid Mechanics and Convective Transport Processes*. Cambridge University Press.

MICHELIN, S. & LAUGA, E. 2011 Optimal feeding is optimal swimming for all Péclet numbers. *Phys. Fluids* **23**, 101901.

MORRISON, F. A. 1970 Electrophoresis of a particle of arbitrary shape. *J. Colloid Interface Sci.* **34**, 210–214.

O'BRIEN, R. W. & WHITE, L. R. 1978 Electrophoretic mobility of a spherical colloidal particle. *J. Chem. Soc. Faraday Trans.* **2** (74), 1607–1626.

OHSHIMA, H., HEALY, T. W., WHITE, L. R. & O'BRIEN, R. W. 1984 Sedimentation velocity and potential in a dilute suspension of charged spherical colloidal particles. *J. Chem. Soc. Faraday Trans.* **80** (10), 1299–1317.

OVERBEEK, J. T. G. 1943 Theorie der Elektrophorese: der Relaxationseffekt. *Kolloid-Beihefte* **54**, 287.

PRIEVE, D. C., EBEL, J. P., ANDERSON, J. L. & LOWELL, M. E. 1984 Motion of a particle generated by chemical gradients. Part 2. Electrolytes. *J. Fluid Mech.* **148**, 247–269.

RUBINSTEIN, I. & ZALTZMAN, B. 2001 Electro-osmotic slip of the second kind and instability in concentration polarization at electrodialysis membranes. *Math. Models Meth. Appl. Sci.* **11**, 263–300.

SAVILLE, D. A. 1977 Electrokinetic effects with small particles. *Annu. Rev. Fluid Mech.* **9**, 321–337.

SCHNITZER, O., KHAIR, A. & YARIV, E. 2011 Irreversible electrokinetic repulsion in zero-Reynolds-number sedimentation. *Phys. Rev. Lett.* **107**, 278301.

SMOLUCHOWSKI, M. 1921 Elektrische Endosmose und Strömungsströme. In *Handbuch der Elektrizität und des Magnetismus, vol. II, Stationäre Ströme* (ed. L. Graetz). Barth.

TABATABAEI, S. M., VAN DE VEN, T. G. M. & REY, A. D. 2006 Electroviscous sphere-wall interactions. *J. Colloid Interface Sci.* **301** (1), 291–301.

https://doi.org/10.1017/jfm.2012.221 Published online by Cambridge University Press

VAN DYKE, M. 1964 *Perturbation Methods in Fluid Mechanics*. Academic.

VAN DE VEN, T. G. M., WARSZYNSKI, P. & DUKHIN, S. S. 1993 Electrokinetic lift of small particles. *J. Colloid Interface Sci.* **157** (2), 328–331.

WARSZYSKI, P., WU, X. & VAN DE VEN, T. 1998 Electrokinetic lift force for a charged particle moving near a charged wall: a modified theory and experiment. *Colloid Surf.* A **140** (1-3), 183–198.

YARIV, E. 2006 Force-free electrophoresis? *Phys. Fluids* **18**, 031702.

YARIV, E. 2010 An asymptotic derivation of the thin-Debye-layer limit for electrokinetic phenomena. *Chem. Engng Commun.* **197**, 3–17.

YARIV, E. & DAVIS, A. 2010 Electro-osmotic flows over highly polarizable dielectric surfaces. *Phys. Fluids* **22**, 052006.

YARIV, E., SCHNITZER, O. & FRANKEL, I. 2011 Streaming-potential phenomena in the thin-Debye-layer limit. Part 1. General theory. *J. Fluid Mech.* **685**, 306–334.

YOSSIFON, G., FRANKEL, I. & MILOH, T. 2007 Symmetry breaking in induced-charge electro-osmosis over polarizable spheroids. *Phys. Fluids* **19**, 068105.

https://doi.org/10.1017/jfm.2012.221 Published online by Cambridge University Press